

Electrochemical Behavior of Ni(II) Complexes with N₂S₂ and N₆ Ligands as Potential Catalysts in Hydrogen Evolution Reaction

Vanessa Ramírez-Delgado,¹ Guadalupe Osorio-Monreal,¹ Luis Felipe Hernández-Ayala,² Yolanda Reyes-Vidal,^{1,3} Juan Carlos García-Ramos,^{2,†} Lena Ruiz-Azuara² and Luis Ortiz-Frade^{1,*}

¹ Centro de Investigación y Desarrollo Tecnológico en Electroquímica S.C. Parque Tecnológico Querétaro, Sanfandila, Pedro de Escobedo, C.P. 76703. Querétaro, México. lortiz@cideteq.mx

² Laboratorio de Química Inorgánica Medicinal. Departamento de Química Inorgánica y Nuclear, Facultad de Química, Universidad Nacional Autónoma de México, Av. Universidad 3000, Ciudad Universitaria, México, D.F., 04510, México

³ Catedra Conacyt -CIDETEQ

† Currently a postdoctoral fellow at Departamento de Fisicoquímica, Instituto de Química, UNAM.

Received October 7th, 2015; Accepted February 17th, 2016.

Abstract. In this work, two Ni(II) complexes with the tetradentate ligand N₂S₂ (*pdto*=1,8-bis(2-pyridyl)-3,6-dithiooctane,) and the hexadentate ligand N₆ (*bdahp*=2,9-bis-(2',5'-diazahexanyl)-1,10-phenanthroline) were prepared in order to explore its electrochemical behavior, that indicate their potential use as molecular catalysts for the hydrogen evolution reaction. The Ni(II)-*pdto* complex presented two consecutive one electron transfer [Ni(II)-(pdto)] + 1e⁻ [Ni(I)-(pdto)] and [Ni(I)-(pdto)] + 1 e⁻ → Ni(0) + pdto. On the other hand the Ni(II)-*bdahp* complex presented the electrochemical reduction Ni(II)-(bdahp) + 1e⁻ Ni(I)-(bdahp) followed by a coupled chemical reaction in an ECi mechanism, where a de-coordination of the diiminic moiety of the *bdahp* ligand was proposed. It was demonstrated that the *pdto* ligand promotes reduction over Ni(II) at less negative reduction potential in comparison when the ligand *bdahp* is presented.

Key words: Electrochemistry, Ni(II) complexes; N₂S₂ ligand; N₆ ligand.

Resumen. En este trabajo se prepararon dos complejos de Ni(II) con un ligante tetradentado N₂S₂ (*pdto*=1,8-bis(2-piridil)-3,6-ditiocatano) y un ligante hexadentado N₆ (*bdahp* = 2,9-bis-(2',5'-diazahexanilo)-1,10-fenantrolina) con el fin de estudiar su comportamiento electroquímico que indique su potencial uso como catalizadores moleculares en la reacción de evolución de hidrógeno. El complejo Ni(II)-*pdto* presenta dos transferencias mono-electrónicas consecutivas [Ni(II)-(pdto)] + 1e⁻ [Ni(I)-(pdto)] y [Ni(I)-(pdto)] + 1 e⁻ → Ni(0) + pdto. Por otro lado el complejo Ni(II)-*bdahp* presentó la reducción electroquímica Ni(II)-(bdahp) + 1e⁻ Ni(I)-(bdahp) seguida de una reacción química acoplada en un mecanismo de ECi, donde se propone una des-coordinación de la parte diimínica del ligante *bdahp*. Se demostró que el ligante *pdto* promueve la reducción del Ni(II) en potencial de reducción menos negativo en comparación cuando está presente el ligante *bdahp*.

Palabras clave: Electroquímica; complejos Ni(II); ligante N₂S₂; ligante N₆.

Introduction

The economic dependence of fossil combustibles has motivated scientists around the world to develop alternative energy sources. The use of solar radiation for water splitting to produce H₂ and O₂, also called artificial photosynthesis, and the electrochemical hydrogen evolution are considered potential strategies for energy storage [1]. Inert electrodes with noble metals, particularly bulk and nanostructured Pt, have been widely used to achieve this goal. Nevertheless coordination compounds present advantages, such as the use of non-expensive metals and the accurate control of chemical reactivity. Typically Co(II)-diglyoxime complexes in non-aqueous solvents with HA proton donors have been used for hydrogen evolution catalysis [2-6]. The low stability of these systems has motivated to explore alternative compounds such as Co(II)-polypyridine complexes and highly competitive Ni(II) complexes [6-10]. DuBois designed the Ni(II) complex [Ni(P^{Ph}₂N^{Ph})₂](BF₄)₂ (P^{Ph}₂N^{Ph}=1,3,6-triphenyl-1-aza-3,6-diphosphacycloheptane, X=OMe, Me, Br, Cl or CF₃, with similarities to the ligand P^{Ph}₂N^{Ph}) were also reported [12-16]. The basicity of the amine in the ligand, and the catalytic activity was modified by the presence of electron donating and electron withdrawing substituents X on the aromatic ring attached to the nitrogen atom. In a biomimetic approach to the Ni-Fe Hydrogenases, ligands with N/S donor atoms, specifically substituted and non-substituted pyridine-2-thiolate and pyrimidine-2-thiolate were also used to prepare Ni(II) complexes, with a decent electro-catalysis and photo-driven hydrogen evolution activities [15-20]. From all these studies it was figured out that in the proposed mechanism, the first step is a one electron uptake over Ni(II), followed by the formation of hydride species Ni(II)-H. From this work, it was established that for a good catalyst, flexible ligands are desirable because of the preferential geometries of the proposed Nickel oxidation states in the catalytic cycle. Another important

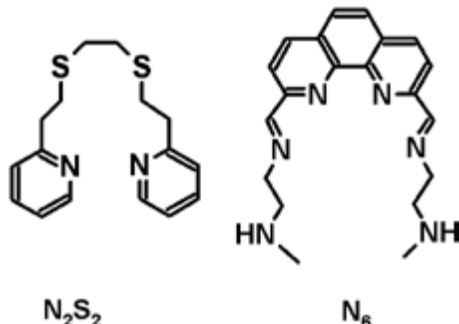
factor is the reduction potential of the couple Ni(II)/Ni(I). A more negative value increases the hydride donor abilities of the Nickel-hydrides, making the process more efficient [12].

A good candidate for a potential hydrogen evolution catalyst is the Ni(II) complex with the ligand 1,8-bis(2-pyridyl)-3,6-dithiaoctane (**pdto**), due to the presence of N/S donor atoms and the already demonstrated high flexibility toward the preferential geometry of a metal center, see scheme 1 [21-40]. On the other hand, the negative reduction potential of Ni(II) coordinated to a diiminic moiety and the flexibility of protonable open chain amines, make that the Ni(II) complex with the ligand 2,9-bis-(2',5'-diazahexanyl)-1,10-phenanthroline (**bdahp**), see scheme 1, can be considered as a possible catalyst for hydrogen evolution reaction. Therefore, in this work we prepared two Ni (II) complexes with flexible ligands N₂S₂ (**pdto**) and (**bdahp**) (**pdto**=1,8-bis(2-pyridyl)-3,6-dithiooctane, **bdahp**= 2,9-bis-(2',5'-diazahexanyl)-1,10-phenanthroline) in order to explore its electrochemical behavior that provides information necessary to propose their potential use as catalysts for hydrogen evolution reaction.

Results and discussion

Characterization of [Ni(pdto)(CH₃CN)₂](BF₄)₂

The reaction between the Nickel salt [Ni(H₂O)₆](BF₄)₂ and the ligand 1,8-bis(2-pyridyl)-3,6-dithiooctane yield a blue powder with empirical formula C₂₀H₂₆N₄S₂B₂F₈Ni. The IR spectrum displays typical adsorption bands for **pdto**. The stretching vibrations from pyridine rings v(C=C) + v(C=N) are recorded at 1608 and 1565 cm⁻¹. The asymmetric stretching v_{as}(CH) and symmetric stretching v_s (CH) are observed at 2855, 2835 and 2819 cm⁻¹. Methylene scissoring bands (δ_s CH₂) occur at 1436 and 1482 cm⁻¹. Sharp absorption bands at 3103 and 3016 cm⁻¹ attributable to aromatic stretching v (=C-H) are also observed. The absorptions bands corresponding to the out of plane δ(=C-H) bending is registered at 770 cm⁻¹. Characteristic signals for coordinated CH₃CN, v(-C-H) and v(C≡N) are recorded at 2950, 2920, 2257 and 2287 cm⁻¹. A broad signal around 1080 cm⁻¹ characteristic for BF₄⁻ anion was observed. With this



Scheme 1. Ligands N₂S₂ (**pdto**)= 1,8-bis(2-pyridyl)-3,6-dithiooctane, and N₆ (**bdahp**) = 2,9-bis-(2',5'-diazahexanyl)-1,10-phenanthroline).

information it is not possible to propose a geometry for the Ni(II) complex. Thus NIR diffuse reflectance spectra was acquired, see fig. 1. Three absorption bands at 10535, 16813 and 26650 cm⁻¹ can be observed, which correspond to the electronic transitions v₁=³A_{2g}(F) → ³T_{2g}(F); v₂=³A_{2g}(F) → ³T_{1g}(F); v₃=³A_{2g}(F) → ³T_{1g}(P) for typical octahedral Ni (II) complexes. These are in agreement with calculated effective magnetic moment (μeff) 2.97 MB (2 unpaired electrons) [41-43]. Additionally a Charge Transfer (CT) absorption band at 30337 and a spin-forbidden electronic transition ³A_{2g} → ¹E_g at 9655 cm⁻¹ were also recorded [44]. A **10 Dq** value of 10535 cm⁻¹ is assigned, according to the literature [45]. The above discussion allows us to propose unequivocally the molecular formula [Ni(**pdto**)(CH₃CN)₂](BF₄)₂.

On the other hand, to explore the geometry of this Ni(II) complex in solution, conductimetric and spectroscopic measurements were performed. A 1 mM solution of the complex in acetonitrile presented a molar conductance (Λ_m) value of 320 Ω⁻¹cm²mol⁻¹, characteristic for a 2:1 electrolyte. The UV-visible spectrum of the compound in acetonitrile shows the electronic transitions v₂=³A_{2g}(F) → ³T_{1g}(F), v₁=³A_{2g}(F) → ³T_{2g}(F), and ³A_{2g} → ¹E_g at 565 nm (17699 cm⁻¹), 880 nm (11360 cm⁻¹) and 936 nm (1070 cm⁻¹) respectively, see fig. 2. These results indicate that the complex present an octahedral geometry with the same donor atoms around the Ni(II) center in acetonitrile solution and in solid state. The slight changes in maximum absorption bands are related to solvation effects.

Characterization of [Ni(bdahp)](PF₆)₂

A purple powder was obtained with empirical formula NiC₂₀H₂₈N₆P₂F₁₂. The presence of the polypyridine 1,10-phenanthroline moiety and aliphatic amines of the **bdahp** ligand are confirmed by IR spectroscopy. The stretching absorption bands v (C=C) + v (C=N) occur at 1591, 1500, 1462 and 1435 cm⁻¹. The aromatic stretching v (=C-H) signals are detected at

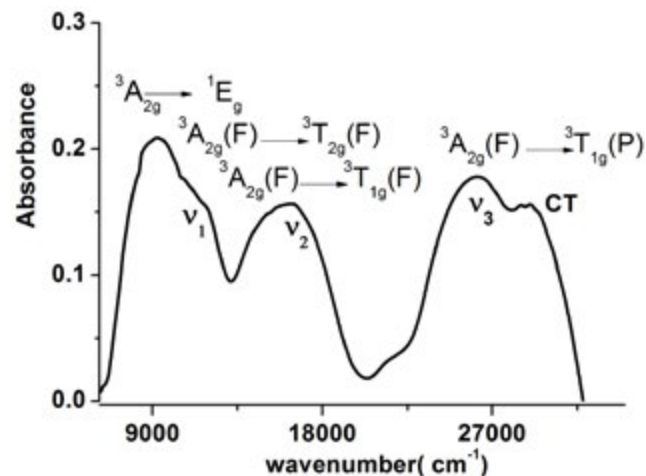


Fig. 1 Typical NIR diffuse reflectance spectra of the complex [Ni(**pdto**)(CH₃CN)₂](BF₄)₂

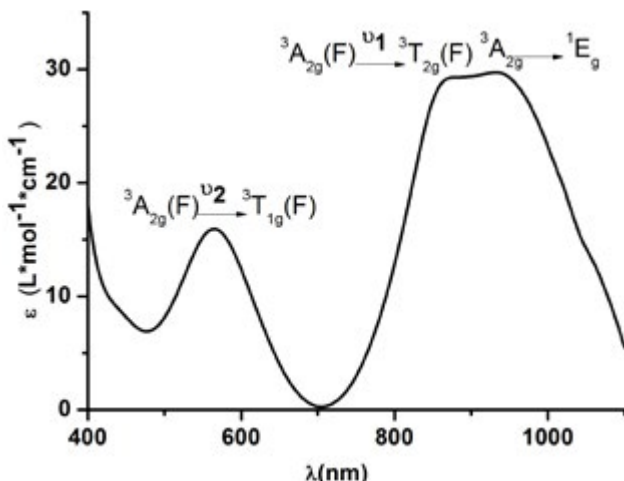


Fig. 2. UV-visible spectrum of the compound $[\text{Ni}(\text{pdto})(\text{CH}_3\text{CN})_2](\text{BF}_4)_2$ 5×10^{-3} M in MeCN solution.

3087 cm^{-1} . The absorptions bands corresponding to the out of plane C-H bending are registered at 743, 723, and 686 cm^{-1} . The (N-H) stretching bands are observed at 3344 and 3323 cm^{-1} . The absorption bands for the stretching ν (-C-H) associated to CH_3 and CH_2 groups are detected at 2997, 2970, 2945 and 2925 cm^{-1} . Moreover the counter ion (PF_6^-) was recorded around 825 cm^{-1} . The electronic spectra of this complex in acetonitrile solution is presented in fig. 3. In the same way that in the Ni(II)-**pdto** complex the effective magnetic moment (μ_{eff}) 3.04 BM and the electronic transitions in acetonitrile solution $v_2 = {}^3\text{A}_{2g}(\text{F}) \rightarrow {}^3\text{T}_{1g}(\text{F})$, $v_1 = {}^3\text{A}_{2g}(\text{F}) \rightarrow {}^3\text{T}_{2g}(\text{F})$ and ${}^3\text{A}_{2g} \rightarrow {}^1\text{E}_g$ at 551 nm (18148 cm^{-1}), 980 nm (10204 cm^{-1}) and 1017 nm (9832 cm^{-1}) demonstrate a octahedral geometry for the Ni(II) complex. The presence of a shoulder (*) around 830 nm, is attributed to electronic transitions for RHN-Ni(II) fragment which has a lower crystal filed splitting according to spectrochemical series [42]. The solution behavior was complemented with conductimetric

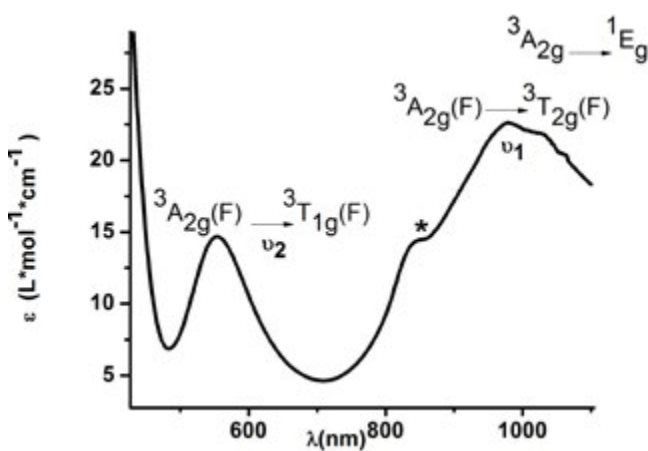


Fig. 3. UV-visible spectrum of the compound $[\text{Ni}(\text{bdahp})](\text{PF}_6)_2$ 0.01 M in MeCN solution.

measurements. The calculated molar conductance value $\Lambda_m = 300 \Omega^{-1}\text{cm}^2\text{mol}^{-1}$ for a 1 mM solution of the complex (2:1 electrolyte) indicates the complete dissociation of the compound that generate the cationic complex and two counterions PF_6^- . This information allows the proposal of molecular formula $[\text{Ni}(\text{bdahp})](\text{PF}_6)_2$.

Electrochemical behavior of $[\text{Ni}(\text{pdto})(\text{CH}_3\text{CN})_2](\text{BF}_4)_2$ in acetonitrile solution

A typical cyclic voltammogram of the complex $[\text{Ni}(\text{pdto})(\text{CH}_3\text{CN})_2](\text{BF}_4)_2$ in acetonitrile solution in the presence of 0.1 M TBABF₄ is shown in fig. 4. When the potential scan was started from open circuit potential to negative direction two reduction processes I_c and II_c and two oxidation processes I_a and II_a were recorded. The corresponding potential peaks for these signals are $E_{pc}(I) = -1.004$ V, $E_{pc}(II) = -1.630$, $E_{pa}(I) = -0.889$ V and $E_{pa}(II) = -0.237$ V vs Fc-Fc⁺. When the scan rate was increased, see fig. 5, the signals I_c , II_c and I_a presented an increment on their corresponding current values. The opposite was registered for signal II_a . It should be highlighted that an increase of current for signals I_a and I_c when the time scale of the experiment was diminished, indicates a dependence between them. To prove this idea cyclic voltammetry experiments using a lower cathodic switching potential value ($E_{-\lambda}$) were carried out. Fig. 6 shows a series of voltammograms at variable scan rate with a $E_{-\lambda}$ value at -1.25 V vs Fc-Fc⁺, where only the redox processes I_c and I_a were observed. The anodic peak potential $E_{pa}(I)$ present a shift from -0.889 (long $E_{-\lambda}$) to -0.924 (short $E_{-\lambda}$) V vs Fc-Fc⁺, meanwhile no change was observed in the cathodic peak potential $E_{pc}(I)$. The ratio $i_{pa}(I_a)/i_{pc}(I_c)$ presents a value close to the unity in the whole range of scan rates. Therefore we propose the electron transfer $\text{Ni}(\text{II})-(\text{pdto}) + 1 e^- \text{Ni}(\text{I})-(\text{pdto})$ for process I, with a half wave potential ($E_{1/2}$) value of -0.964 V vs Fc-Fc⁺ and a difference between potential peaks (ΔE_p)

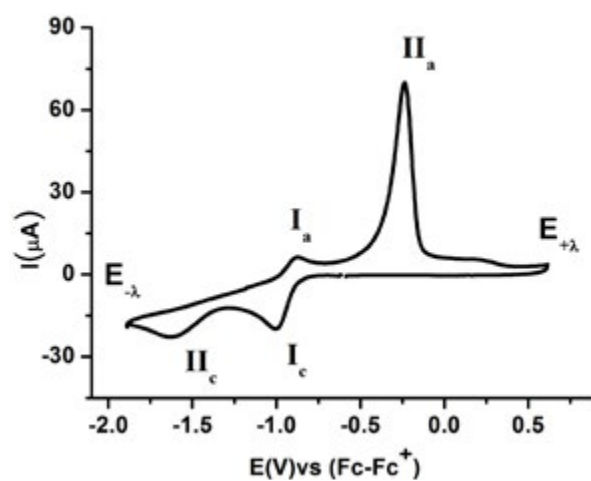


Fig. 4. Cyclic voltammogram for 1×10^{-3} M of $[\text{Ni}(\text{pdto})(\text{CH}_3\text{CN})_2](\text{BF}_4)_2$ in the presence of 0.1 M TBABF₄ in MeCN, obtained with a glassy carbon disk as working electrode. Scan rate 100 mV s⁻¹

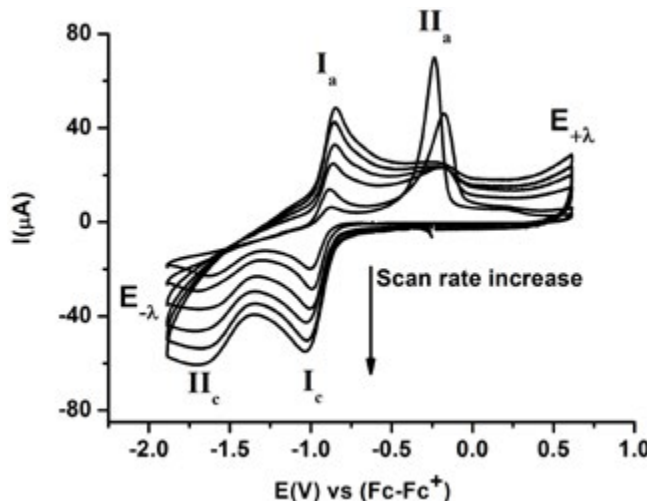


Fig. 5. Cyclic voltammogram for 1×10^{-3} M of $[\text{Ni}(\text{pdto})(\text{CH}_3\text{CN})_2](\text{BF}_4)_2$ in the presence of 0.1 M TBABF₄ in MeCN, obtained with a glassy carbon disk as working electrode. Scan rate from 100 to 1000 mVs⁻¹

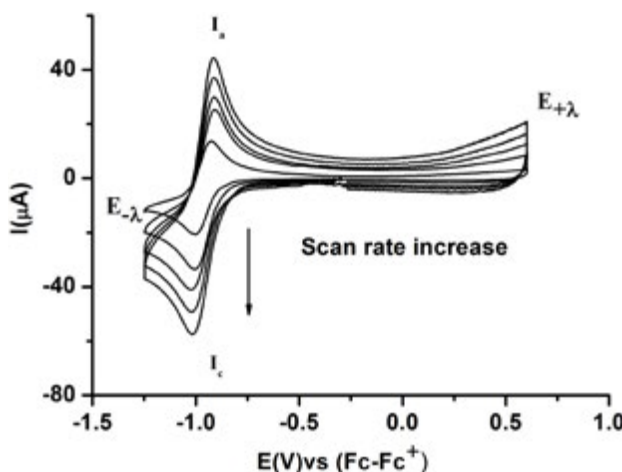


Fig. 6. Cyclic voltammogram for 1×10^{-3} M of $[\text{Ni}(\text{pdto})(\text{CH}_3\text{CN})_2](\text{BF}_4)_2$ in the presence of 0.1 M TBABF₄ in MeCN, obtained with a glassy carbon disk as working electrode. Scan rate from 100 to 1000 mVs⁻¹. Cathodic switching potential value ($E_{-\lambda}$) at -1.25 V vs Fc-Fc⁺.

close to 0.080 V. Considering the assignation for process I and cyclic voltamograms, it was possible to attribute signal II_c to the electrochemical reaction $\text{Ni(I)-(pdto)} + 1 e^- \rightarrow \text{Ni(0)} + \text{pdto}$, and process II_a to the anodic dissolution of Ni(0) deposited in the forward scan. This fact explain the change in the anodic peak potential values E_{pa} for process I_a when the switching was modified, in terms of different energetic requirements for the oxidation of the Ni(I)-(pdto) species over glassy carbon (short $E_{-\lambda}$) and over a Ni(0) deposit (long $E_{-\lambda}$). One step chronoamperometry experiment stepped from open circuit potential ($E_{i=0}$) to potential value $E_1 = -1.247$ V vs Fc-Fc⁺ with a perturbation time $\tau = 1$ s, allows to calculate a diffusion coefficient of $1.443 \times 10^{-5} \text{ cm}^2 \text{ s}^{-1}$ according to Cottrell's law [46, 47].

Electrochemical behavior of $[\text{Ni}(\text{bdahp})_3](\text{PF}_6)_2$ in acetonitrile solution

The cyclic voltammogram of compound $[\text{Ni}(\text{bdahp})_3](\text{PF}_6)_2$ obtained with a glassy carbon electrode at scan rate $v=100$ mV s⁻¹ in acetonitrile solution is shown in fig. 7. In the complete scan (started from open circuit potential to negative direction) the voltammogram displays two oxidation signal I_a and II_a with their corresponding reduction signal I_c and II_c. For process I a half-wave potential ($E_{1/2}$) value of 1.013 V/Fc-Fc⁺ and a ΔE_p value of 0.060 V value was obtained. On the other hand for process II their corresponding ΔE_p and $E_{1/2}$ values were 0.060 V and -1.832 V/Fc-Fc⁺ respectively. In order explain the nature of both electron transfers, the electrochemical study of the complex $[\text{Ni}(1,10\text{-phen})_3](\text{BF}_4)_2$ in the same experimental conditions was carried out. One oxidation process with a half wave potential $E_{1/2} = 1.419$ V vs Fc-Fc⁺ associated to $[\text{Ni}^{\text{II}}(1,10\text{-phen})_3]^{2+} [\text{Ni}^{\text{III}}(1,10\text{-phen})_3]^{3+} + 1e^-$ was observed [48, 49]. A second process associated to the reduction $[\text{Ni}^{\text{II}}(1,10\text{-phen})_3]^{2+} + 1e^- [\text{Ni}^{\text{I}}(1,10\text{-phen})_3]^+$ with a half wave potential $E_{1/2} = -1.629$ V vs Fc-Fc⁺ was also detected. Taking into account similar oxidizable and reducible groups between $[\text{Ni}(\text{bdahp})]^{2+}$ and it was possible to establish the electrochemical reactions; $[\text{Ni}^{\text{II}}(\text{bdahp})]^{2+} [\text{Ni}^{\text{III}}(\text{bdahp})]^{3+} + 1e^-$ for process I and $[\text{Ni}^{\text{II}}(\text{bdahp})]^{2+} + 1e^- [\text{Ni}^{\text{I}}(\text{bdahp})]^+$ for process II. This is in agreement with the fact that imine ligands such as 1,10-phen and bipyridine offer a more attractive environment for Ni(I) and other metal complexes in low oxidation state by allowing electron delocalization over the ligand π system [49-55]. When the scan rate was increased the corresponding cyclic voltammograms showed a better definition of the oxidation signal II_a with an increment in its current value. The ratio $i_{pa}(\text{II}_a)/i_{pc}(\text{II}_c)$ presented small values at low scan rate, characteristic of a coupled chemical reaction in an ECi mechanism, see fig. 8. In literature it has been stated that the electrochemical reduction for the cationic complexes $[\text{Ni}^{\text{II}}\text{L}_3]^{2+}$ ($\text{L}=1,10\text{-phen}$, and bipyridine) in anhydrous acetonitrile results in $[\text{Ni}^{\text{I}}\text{L}_2]^{2+}$ [49, 56, 57]. Based

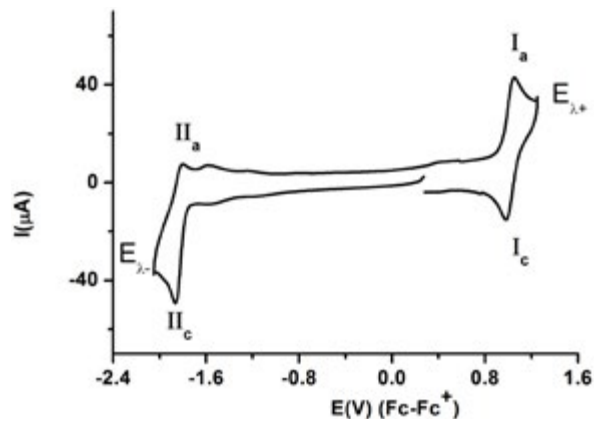


Fig. 7. Cyclic voltammogram for 1×10^{-3} M $[\text{Ni}(\text{bdahp})](\text{PF}_6)_2$ in the presence of 0.1 M TBABF₄ in MeCN, initiated from open circuit potential to positive direction. The working electrode was a glassy carbon disk. Scan rate 100 mVs⁻¹.

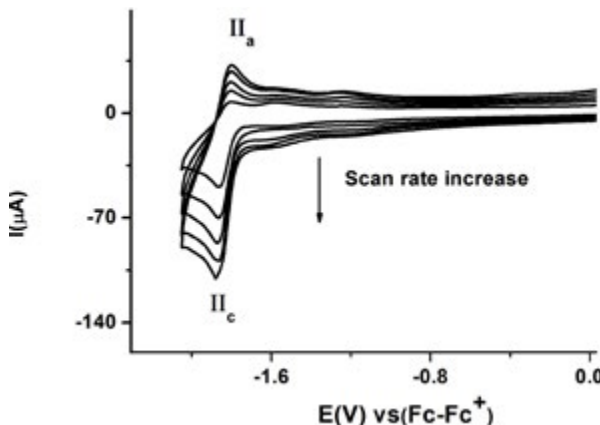


Fig. 8. Cyclic voltammogram for 1×10^{-3} M $[\text{Ni}(\text{bdahp})](\text{PF}_6)_2$ in the presence of 0.1 M TBABF₄ in MeCN, initiated from open circuit potential to negative direction. The working electrode was a glassy carbon disk. Scan rate from 100 to 1000 mVs⁻¹.

on this fact we can propose a de-coordination of the diiminic moiety of the **bdahp** ligand with the electrogenerated Ni(I) forming the species $[\text{Ni}(\kappa^4\text{N}-\text{bdahp})]^+$, detectable in the time scale of the cyclic voltammetry employed. According to the literature the rate constant (k_f) for the EC_i mechanism was calculated [58,59]. The obtained values were 0.160 ± 0.007 and 0.170 ± 0.001 for compounds $[\text{Ni}(1,10\text{-phen})_3]^{2+}$ and $[\text{Ni}(\text{bdahp})]^{2+}$ respectively. The low value for the 1,10-phen complex in comparison with the **bdahp** complex is related to high chelate effect.

From one step chronoamperometry experiments, with a potential step from open circuit potential to -1.90 vs Fc-Fc⁺, a diffusion coefficient of 7.97×10^{-5} cm²s⁻¹ was calculated according to Cottrell law. Similar experiments were performed for the complex $[\text{Ni}(1,10\text{-phen})_3]^{2+}$ stepping the potential to -1.80 vs Fc-Fc⁺ ($D_{\text{o}} = 3.48874 \times 10^{-5}$ cm²s⁻¹)

Comparison of the electrochemical behavior of Ni(II) complexes

Fig. 9 presents a graphical comparison of the electrochemical reductions of the compounds studied in this work. From this figure it can be established that the Ni(II) complex with the ligand N₆ $[\text{Ni}(\text{bdahp})]^{2+}$ which contains a diiminic moiety and flexible aliphatic amines the redox potential is shifted to more negative values in comparison with the $[\text{Ni}(\text{pdto})(\text{CH}_3\text{CN})_2]^{2+}$ complex. The change in denticity of a bidentate ligand (1,10-phenanthroline) to a hexadentate ligand N₆ **bdahp**=2,9-bis-(2',5'-diazahexanyl)-1,10-phenanthroline causes that the reduction of Ni(II) requires more energy, despite the fact that the tris-chelate $[\text{Ni}(1,10\text{-phen})_3]^{2+}$ complex should present a more negative reduction potential, according to the additivity contribution of three ligands with high π acceptor character [60]. Hence this shift in reduction potential could be attributable to the chelate effect. An important change in the diffusion coefficient could be observed, as a consequence of the molecular size of the cationic complexes considering the solvation

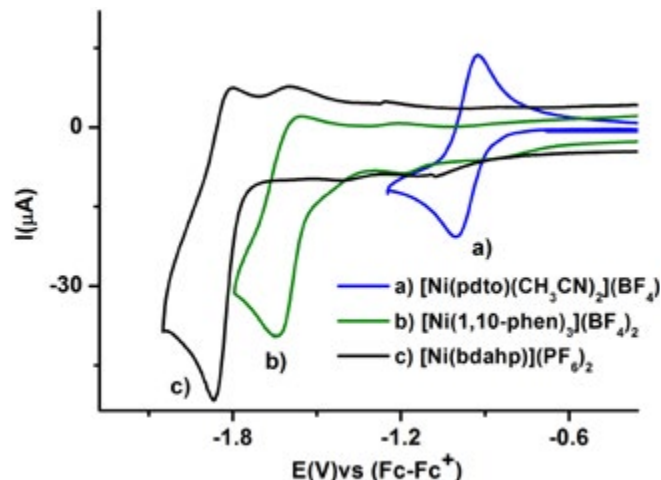


Fig. 9. Comparison of cyclic voltammogram for the compounds 1mM a) $[\text{Ni}(\text{pdto})(\text{MeCN})_2](\text{BF}_4)_2$, b) $[\text{Ni}(\text{bdahp})](\text{PF}_6)_2$ and c) $[\text{Ni}(1,10\text{-phen})_3](\text{BF}_4)_2$ in the presence of 0.1 M TBABF₄ in MeCN, initiated from open circuit potential to negative direction. The working electrode was a glassy carbon disk. Scan rate from 100 mVs⁻¹.

sphere of each compound. Table 1 shows a summary of the electrochemical reduction processes of the compounds studied in this work, and other Ni(II) complexes used for electrochemical hydrogen evolution taken from literature.

The complex $[\text{Ni}(\text{bdahp})]^{2+}$ presented a more negative reduction potential (-1.83 vs Fc-Fc⁺) than those reported for Ni(II) complexes with ligands containing phosphorus donor atoms on its structure $[\text{Ni}(\text{PPh}_2\text{N}^{\text{Ph}}_2)_2]^{2+}$ ($\text{PPh}_2\text{N}^{\text{Ph}} = 1,3,6\text{-triphenyl-1-aza-3,6-diphosphacycloheptane}$) and $[\text{Ni}(7\text{PPh}_2\text{N}^{\text{C}_6\text{H}_4\text{X}}_2)]^{2+}$ ($7\text{PPh}_2\text{N}^{\text{C}_6\text{H}_4\text{X}} = 1\text{-para-X-phenyl-3,6-triphenyl-1-aza-3,6-diphosphacycloheptane}$, X= OMe, Me, Br, Cl or CF₃) (from -1.13 to 1.05 vs Fc-Fc⁺). Considering that a negative redox potential value increases the hydride donor ability, making the hydrogen evolution reaction more efficient, a good catalytic activity for the complex $[\text{Ni}(\text{bdahp})]^{2+}$ is expected. On the other hand the reduction potential (-0.96 vs Fc-Fc⁺) of the cationic complex $[\text{Ni}(\text{pdto})(\text{MeCN})_2]^{2+}$ suggests a low hydride donor ability in comparison with the reported values for the bioinspired Ni(II) complexes with N/S ligands $[\text{Ni}(\text{X-pyS})_3]$, $[\text{Ni}(\text{pySH})_4]^{2+}$, $[\text{Ni}(4,6\text{-Y}_2\text{-pymS})_3]$ and $[\text{Ni}(4,4'\text{-Z-2,2'-bpy})(\text{pyS})_2]$ (pyS = pyridine-2-thiolate, X= H, CH₃, Z= H, CH₃, OCH₃ and bpy = bipyridine) (from -1.73 to 2.01 vs Fc-Fc⁺). However the Ni(II)-**pdto** system presented a necessary reversible electron transfer Ni(II) + 1 e⁻ Ni(I) in a catalytic cycle, which is not observed in the Ni(II) complexes with substituted and non-substituted pyridine-2-thiolate, pyrimidine-2-thiolate and 4,4'-bipyridines, see table 1.

Conclusions

Using typical characterization techniques octahedral Ni(II) complexes with the tetradentate ligand N₂S (**pdto**=1,8-bis

Table 1. Electrochemical reduction processes for Ni(II) complexes studied in this work with their corresponding half wave redox potential (E_{1/2}). Data of other Ni(II) used for hydrogen evolution reaction taken from literature is also presented.

Electrochemical processes	E _{1/2} (V)
[Ni(II)-(pdto)] + 1e ⁻ [Ni(I)-(pdto)]	-0.96
[Ni(I)-(pdto)] + 1 e ⁻ → Ni(0) + pdto	-1.63 ^a
[Ni ^{II} (1,10-phen) ₃] ²⁺ +1e [Ni ^I (1,10-phen) ₃] ⁺	-1.63
[Ni ^{II} (bdahp)] ²⁺ +1e [Ni ^I (bdahp)] ⁺	-1.83
[Ni ^{II} (PPh ₂ N ^{Ph}) ₂] ²⁺ +2e [Ni ^I (PPh ₂ N ^{Ph}) ₂]	-1.13
[Ni ^{II} (7PPh ₂ N ^{C6H4OMe}) ₂] ²⁺ +2e [Ni ^I (7PPh ₂ N ^{C6H4OMe}) ₂]	-1.14
[Ni ^{II} (7PPh ₂ N ^{C6H4Me}) ₂] ²⁺ +2e [Ni ^I (7PPh ₂ N ^{C6H4Me}) ₂]	-1.13
[Ni ^{II} (7PPh ₂ N ^{Ph}) ₂] ²⁺ +2e [Ni ^I (7PPh ₂ N ^{Ph}) ₂]	-1.12
[Ni ^{II} (7PPh ₂ N ^{C6H4Br}) ₂] ²⁺ +2e [Ni ^I (7PPh ₂ N ^{C6H4Br}) ₂]	-1.08
[Ni ^{II} (7PPh ₂ N ^{C6H4Cl}) ₂] ²⁺ +2e [Ni ^I (7PPh ₂ N ^{C6H4Cl}) ₂]	-1.08
[Ni ^{II} (7PPh ₂ N ^{C6H4CF₃}) ₂] ²⁺ +2e [Ni ^I (7PPh ₂ N ^{C6H4CF₃}) ₂]	-1.05
[Ni(6-CH ₃ -Pyridine-2-thiolate) ₃] ⁻ +ne → P	-1.72 ^{a,b}
[Ni(HPyridine-2-thiolate) ₄] ²⁺ +ne → P	-1.78 ^{a,b}
[Ni(2,2'-bpy)(pyridine-2-thiolate) ₂] ⁺ +ne → P	-1.93 ^{a,b}
[Ni(4,4'-dimethyl-2,2'-bpy)(pyridine-2-thiolate) ₂] ⁺ +ne → P	-2.02 ^{a,b}
[Ni(2,2'-dimethoxy-bpy)(pyridine-2-thiolate) ₂] ⁺ +ne → P	-2.06

Reported vs Fc-Fc⁺, scan rate 100 mVs⁻¹ in 0.1 M TBABF₄ in MeCN.^a Irreversible process, cathodic peak value.^b Reported in DMF.

(2-pyridyl)-3,6-dithiooctane,) and the hexadentate ligand N₆ (**bdahp** = 2,9-bis-(2',5'-diazahexanyl)-1,10-phenanthroline) are proposed . The cationic complexes [Ni(**pdto**)(CH₃CN)₂]²⁺ and [Ni(**bdahp**)]²⁺ presented an electron transfer from Ni(II) to Ni(I), with half wave redox potential controlled by donor atoms. It was demonstrated that the coordination of a N₂S₂ ligand with Ni(II) makes the reduction potential shift to less negative values in comparison to Ni(II) complexes with a N₆ ligand **bdahp**. The electrochemical behavior, through an analysis of the reduction potential values of [Ni(**pdto**)(CH₃CN)₂]²⁺ and [Ni(**bdahp**)]²⁺ suggest that both complexes can be considered as potential catalysts for hydrogen evolution reaction in a future work.

Experimental section

Chemicals

All chemicals and solvents in this work were used as received from Aldrich Chemical Co., Acros Organics and J.T. Baker.

Synthesis of the ligand 1,8-Bis(2-pyridyl)-3,6-dithiooctane (**pdto**)

The ligand 1,8-bis(2-pyridyl)-3,6-dithiooctane (**pdto**) was prepared using the method described by Goodwin and Lions. [21]. Yield 70%, elemental analysis calculated for C₁₆H₂₀N₂S₂: calculated %C 63.1, %H 6.6, %N 9.2, %S 21.1; found: %C 63.1, %H 6.2, %N 9.7, S 20.5.

Synthesis of the ligand 2,9-Bis-(2',5'-diazahexanyl)-1,10-phenanthroline (**bdahp**)

12.71 mmol of 2,9-diformyl-1,10-phenanthroline was dissolved in 200 mL of a (1 : 1) mixture CHCl₃-MeOH. Separately 38.15 mmol of N-methyl-ethylenediamine was added to 50 mL of the CHCl₃-MeOH mixture, to be added to the first solution. The reaction mixture was heated and stirred under reflux for 2 hours. When the reaction mixture was cooled at room temperature, 50.84 mmol of the reducing agent NaBH₄ was added. The new reaction mixture was stirred again for 2 hours and a green solution was obtained. Extractions with CHCl₃ were done and the organic phase was collected to be concentrated and re-disolved in 5 mL of concentrated hydrochloric acid with the addition of EtOH. A pale yellow product was obtained filtered and dried. Anal. Calc. for C₂₀H₃₂N₆Cl₄ (M.W.= 498.32 g mol⁻¹) %C, 47.79; %H, 6.52; %N, 17.23. Found: %C, 48.0, %H 6.47; %N 16.86. ¹H-NMR (300 MHz, D₂O) δ 7.53 (d, J= 8.35, 1H), 6.88 (d, J=8.36 Hz, 1H), 6.84 (s, 1H), 3.83 (s, 2H), 2.64 (dd, J1= 8.15, J2= 6.05 Hz, 2H), 2.51 (dd, J1= 8.31, J2= 6.46 Hz, 2H), 1.7 (s, 3 H). ¹³C-NMR (300 MHz, D₂O) δ= 151, 143, 139, 129, 127, 123, 52, 44, 43, 33.

Synthesis of the complexes

[Ni(**pdto**)(CH₃CN)₂](BF₄)₂. The synthesis was carried out by dissolving 2 mmol of the metallic salt Ni(BF₄)•6H₂O in 25 mL of acetonitrile. Then it was added dropwise the metallic salt solution 2 mmol of **pdto** dissolved in 5 mL of acetonitrile. A color change from green to blue was observed. The reaction

mixture was heated and stirred for 2 hours. Solvent was removed by slow evaporation until a blue powder was observed. The product was filtered and washed with ethyl ether. Elemental analysis for $C_{20}H_{26}N_4S_2B_2F_8Ni$ (P. M.=618.87 g mol⁻¹); Calc.: %C 38.81, %H 4.23, %N 9.05, %S 10.36; Found: %C 38.81, %H 4.23, %N 9.05, %S 10.36. Am (MeCN): 320 Ω⁻¹ cm² mol⁻¹. μ_{eff}: 2.907 BM (2 unpaired electrons).

[Ni(1,10-phenanthroline)₃](BF₄)₂. This synthesis was carried out by mixing 1 mmol of Ni(BF₄)₂ • 6H₂O (1×10^{-3} M), dissolved in 20 mL of CH₃OH with 3 mmol of the ligand previously dissolved in CH₃OH. A color solution change from green to pale pink was observed. The reaction mixture was stirred at room temperature for 1 hour. The solvent was removed and a pale pink precipitate was obtained to be filtered and washed with ether.

[Ni(bdahp)](PF₆)₂. 10 mL of aqueous solution containing 1 mmol of [H₄(bdahp)]Cl₄ were added to 15 mL containing 1 mmol of NiCl₂ in aqueous solution. The pH of the solution was adjusted with NaOH. The reaction mixture was stirred for 2 hours. After this time a saturated solution of TBABF₄ was added. A pale purple precipitate was obtained. The product was filtered and washed with ethyl ether. Anal. Calc. for NiC₂₀H₂₈N₆P₂F₁₂ (M.W. = 701.01 g mol⁻¹) %C, 34.26; %H, 4.03; %N, 12.06. Found: %C, 33.97; %H, 3.99; %N, 12.06. Λ(MeOH) = 222.6 cm² ohm⁻¹ mol⁻¹. μ_{eff} = 3.04 BM

Physical measurements

Elemental analysis of the compounds was performed with a Fissons Instruments Analyzer model EA 1108, using a sulfanilamide standard for the equipment calibration. Magnetic susceptibility measurements were obtained with Magnetic Balance Johnson Matthey MSB-1. Solid state UV-vis-NIR spectra were acquired with a Cary-5E Varian spectrophotometer 40000-4000 cm⁻¹. IR, spectra were obtained with a Thermo-Nicolet AVATAR 320 FT-IR 400-4000 cm⁻¹, in transmittance mode on KBr disk. Solution electronic spectra was recorded with Thermo-Scientific Evolution Array spectrophotometer (200-1100 nm), using a quartz cell (l=1cm). Conductivity measurements were obtained with Corning Pinacle 524 conductimeter (cell constant= 1 cm⁻¹). A VARIAN Unity Inova spectrometer was used to record NMR spectra, 1H (300 MHz) and 13C (75.5 MHz) and 13C (75.5 MHz). TMS was used as a reference; CD₃Cl₃-D₃COD was used as solvent

Electrochemical experiments

Electrochemical experiments were performed with a potentiostat/galvanostat Biologic SP-50 using 1×10^{-3} M of each Ni(II) compound in acetonitrile solution + 0.1M 0.1 M TBABF₄. A three cell array was used; working electrode, glassy carbon ($\phi=3$ mm), counter electrode a platinum wire and as pseudo-reference a silver wire. Before each experiment the solutions were bubbled with N₂, and the working electrode was cleaned by polishing its surface with α Alumina (0.3 μm), to be washed with water and sonicated. The potentials are reported vs the

couple Fc/Fc⁺ according to the IUPAC convention [61]. Cyclic voltammetry was performed from open circuit potential to negative direction with variable scan rate from 100 to 1000 mVs⁻¹. IR compensation was applied using the current interrupt method. Single pulse cronoamperometry experiments were obtained stepping the potential from open circuit potential to a potential value where the electrochemical process was limited by diffusion, established from CV experiments. A time width (τ) of 1s was used.

Acknowledgement

The authors thank CONACyT (130500), UNAM-PAPIIT (217613) and UNAM-PAIP (3590-19) for financial support; VRD, and JCGR thank CONACyT and RED FARMED/CONACyT for the scholarships.

References

- Berardi, S.; Drouet, S.; Francàs, L.; Gimbert-Suriñach, C.; Guttentag, M.; Richmond, C.; Stolla, T.; Llobet, A., *Chem. Soc. Rev.*, **2014**, *43*, 7501-7519.
- Eckenhoff, W.T.; McNamara, W.R.; Du, P.; Eisenberg, R., *Biochim. Biophys. Acta*, **2013**, *1827*, 958-973.
- Losse, S.; Vos, J.G.; Rau, S., *Coord. Chem. Rev.*, **2010**, *254*, 2492-2504.
- Dempsey, J. L.; Brinschwin, B.S.; Winkler, J. R.; Gray, H. B., *Accounts Chem. Res.*, **2009**, *42*, 12, 1995-2004.
- Du, P.; Schneider, J. ; William, G.L. ; Brennesel, W. ; Eisenberg R., *J. Am. Chem. Soc.*, **2009**, *48*, 4952-4962.
- Jacques, P.-A.; Artero, V.; Pécaut, J.; Fontecave, M., *P. Nat. Acad. Sci. USA*, **2009**, *106*, 49, 20627-20632.
- Tong, L.; Kopecky, A.; Zong, R.; Gagnon, K.J.; Ahlquist, M.S.G.; Thummel, R.P., *Inorg. Chem.*, **2015**, *54*, 7873-7884.
- Sasaki, Y.; Kato, H.; Kudo, A., *J. Am. Chem. Soc.*, **2013**, *135*, 5441-5449.
- Queyriaux, N.; Jane, R.T.; Massin, J.; Artero, V.; Chavarot-Kerlidou, M.; Queyriaux N., *Coord. Chem. Rev.*, **2015**, *46*, 1-17.
- Chen, X.; Ren, H.; Peng, W.; Zhang, H.; Lu, J.; Zhuang, L., *J. Phys. Chem.*, **2014**, *118*, 20791-20798
- Helm, M.L.; Stewart, M.P. ; Bullock, R.M.; DuBois, M.R.; DuBois, D.L., *Science* **2011**, *333*, 863-866
- DuBois, D. L., *Inorg. Chem.*, **2014**, *53*, 3935-3960.
- Stewart, M. P.; Ho, M-H.; Wiese, S.; Lindstrom, M.L.; Thogerson, C.E.; Raugei, S.; Bullock, R.M.; Helm, M.L., *J. Am. Chem. Soc.* **2013**, *135*, 6033-6046.
- Gross, M.A.; Reynal, A.; Durrant, J.R.; Reisner, E., *J. Am. Chem. Soc.*, **2014**, *136*, 356-366.
- Thoi, V.S.; Sun, Y.; Long, J.R.; Chang, C.J., *Chem. Soc. Rev.*, **2013**, *42*, 2388.
- Eckenhoff, W.T.; Eisenberg, R.; *Dalton Trans.*, **2012**, *41*, 13004-13021.
- Han, Z.; Shen, L.; Brennessel, W.W.; Holland, P.L.; Eisenberg, R., *J. Am. Chem. Soc.*, **2013**, *135*, 14659-14669.
- Das, A.; Han, Z.; Brennessel, W.W.; Holland, P.L.; Eisenberg, R., *ACS Catal.*, **2015**, *5*, 1397-1406.
- Xu, You; Xu, R., *Appl. Sur. Sci.*, **2015**, *351*, 779-793.

20. Wang, M.; Han K.; Zhang, S.; Sun L., *Coord. Chem. Rev.*, **2015**, 287, 1-14.
21. Goodwin, H.A.; Lions, F., *J. Am. Chem. Soc.*, **1960**, 82, 5013-5023.
22. Brubaker, G.R.; Brown, J.N.; Yoo, M.K.; Kinsey, R.A.; Kutchan, T.M.; Mottel, E.A., *Inorg. Chem.*, **1979**, 18, 299-302.
23. Manzanera Estrada, M.; Flores-Alamo, M.; Grevy, M., J.-M.; Ruiz-Azuara, L.; Ortiz-Frade, L.; *Acta Crystallogr. E*, **2012**, 68, m135.
24. Ortiz-Frade, L.; Manríquez, J.; González, I.; Moreno-Esparza, R.; Ruiz-Azuara, L., *Polyhedron*, **2010**, 29, 328-332.
25. Ortiz-Frade, L.A.; Ruiz-Ramírez, L.; González, I.; Marín-Becerra, A.; Alcarazo, M.; Alvarado-Rodríguez, J.G.; Moreno-Esparza, R., *Inorg. Chem.*, **2003**, 42, 1825-1834.
26. Popovitch, J.M.; Addison, A.W.; Butcher, R.J.; Prushan, M.J., *J. Chem Crystallogr.*, **2012**, 42, 295-298.
27. Castineiras, A.; Paredes, M.; Hiller, W., *Acta Crystallogr. Sect. C: Cryst. Struct. Commun.*, **1984**, 40, 2078-2079.
28. Castineiras, A.; Hiller, W.; Strahle, J.; Paredes, M.; Sordo, J., *Acta Crystallogr. Sect. C: Cryst. Struct. Commun.*, **1985**, 41, 41-43.
29. Kolotilov, S.V.; Goreshnik, E.A.; Pavlishchuk, V.V.; Yatsimirskii, K.B., *Russ. J. Inorg. Chem.*, **2000**, 45, 967-975.
30. Castineiras, A.; Diaz, G.; Florencio, F.; García-Blanco, S.; Martínez-Carrera, S.J., *Cristallogr. Spectrosc. Res.*, **1988**, 18, 395-401.
31. Castineiras, A.; Diaz, G.; Florencio, F.; García-Blanco, S.; Martínez-Carrera, S., *Z. Anorg. Allg. Chem.*, **1988**, 101-110, 567.
32. Humphrey, D.G.; Fallon, G.D.; Murray, K.S., *J. Chem. Soc. Commun.*, **1988**, 1356-1358.
33. Rajendiran, V.; Murali, M.; Suresh, E.; Sinha, S.; Somasundaram, K.; Palaniandavar, M., *Dalton Trans.*, **2008**, 1, 148-163.
34. Castineiras, A.; Molleda, C.; Masaguer, J.R.; Coto, V., *Transition Met. Chem.*, **1984**, 8, 129-131.
35. Ramírez-Delgado, V.; Morales León, R.E.; Hernández-Ayala, L.F.; Ramírez Coutiño, V.A.; Rodríguez, F.J.; Osorio-Monreal, G.; García-Ramos, J.C.; Flores-Alamo, M.; Ruiz-Azuara, L.; Ortiz-Frade, L., *Polyhedron*, **2014**, 74, 72-78.
36. Pavlishchuk, V.V.; Kolotilov, S.V.; Michael, E.S.; Prushan, J.; Addison, A.W., *Inorg. Chim. Acta*, **1998**, 278, 217-222.
37. Pavlishchuk, V.V.; Kolotilov, S.V.; Addison, A.W.; Sinn, E.; Prushan, M.J., *Russ. J. Inorg. Chem.*, **2000**, 45, 544-550.
38. Bermejo, E.; Castineiras, A.; Dominguez, R.; Strahle, J.; Hiller, W., *Acta Crystallogr. Sect. C: Cryst. Struct. Commun.*, **1993**, 49, 324-326.
39. Worrell, J.H.; Genova, J.J.; Dubois, T.D. *J. Inorg. Nucl. Chem.*, **1978**, 40, 441-446.
40. Bermejo, E.; Castiñeiras, A.; Domínguez, A.R.; Strähle, J.; Hiller, W., *Acta Crystallogr. C*, **1993**, 49, 1918-1920.
41. Cotton, F.A.; Wilkinson, G., Advanced Inorganic Chemistry, John Wiley and Sons 5th ed., New York, 1988.
42. Huheey, J. E.; Keiter, E. A.; Keiter, R. L., Inorganic Chemistry. 4th ed., Harper Collins College Editions, New York, 1999.
43. Lever A.B. P., *Inorg. Chem.*, **1990**, 29, 1271-1285.
44. Stranger, R; McMahon, K.L; Gahan, L.R.; Bruce, J.I.; Hambley, T.W. *Inorg. Chem.* **1997**, 36, 3466-3475.
45. D. Sutton, *Electronic Spectra of Transition Metal Complexes*. McGraw Hill, **1968**, London, Great Britain.
46. Bard, A.J.; Faulkner, L.R., *Electrochemical Methods, Fundamentals and Applications*. 2nd ed, John Wiley and Sons, New York, 2001.
47. Kissinger, P. T. and Heineman, W. R., *Laboratory Techniques in Electroanalytical Chemistry*, Marcel Dekker, Inc. New York, USA, 1996.
48. Zanello, P., Inorganic Electrochemistry, theory, practice and application, The Royal Society of Chemistry, Cambridge, UK, 2003.
49. Lappin A. Graham; McAuley Alexander The redox chemistry of Nickel, 281-295.
50. Tokel-Takvoryan, N.E.; Hemingway, R. E.; Bard, A. J., *J. Am. Chem. Soc.*, **1973**, 95, 6582-6589.
51. Tanaka, N.; Sato, Y., *Bull. Chem. Soc. Jap.*, **1968**, 41, 2059-2064.
52. Margel, S.; Smith, W.; Anson, F.C. *J. Electrochem. Soc.*, **1978**, 125, 241-246.
53. Tanaka, N.; Sato, Y., *Inorg. Nucl. Chem. Lett.*, **1968**, 4, 487-490.
54. Tanaka, N.; Sato, Y., *Inorg. Nucl. Chem. Lett.*, **1966**, 2, 359-362.
55. Tanaka, N.; Sato, Y., *Electrochim. Acta.*, **1968**, 335-346.
56. Christensen P.A.; Hamnett A.; Higgins S.J.; Timney, J. A., *J. Electroanal. Chem.*, **1995**, 395, 195-209.
57. Salvatore, D.; Paolo, U., *J. Electroanal. Chem.*, **1987**, 219, 259-271.
58. Nicholson, R. S., *Anal. Chem.* **1965**, 37, 1351-1355.
59. Perpone, S.P.; Kretlow, W.J., *Anal. Chem.* **1966**, 38, 1760-1763.
60. Solomon, E.I.; Lever A.P.B., Inorganic Electronic Structure and Spectroscopy, Volume II: Applications and Case Studies, Wiley, New York, 1999, 255-262.
61. Gritzner, G. and Küta J., *Pure Appl. Chem.*, **1984**, 4, 461-466.